

Radiochimica Acta 50, 11–18 (1990)  
© R. Oldenbourg Verlag, München 1990 – 0033-8230/90 \$3.00+0.00

## Determination of Cross Sections for the Production of ${}^7\text{Be}$ , ${}^{10}\text{Be}$ and ${}^{22}\text{Na}$ by High-Energy Protons

By B. Dittrich, U. Herpers

Abteilung Nuklearchemie, Universität zu Köln, FRG;

M. Lüpke, R. Michel

Zentraleinrichtung für Strahlenschutz, Universität Hannover, FRG;

H. J. Hofmann and W. Wölfli

Institut für Mittelenergiephysik, ETH Zürich, Ch

*Dedicated to Professor G. Stöcklin on the occasion of his 60th birthday*

(Received October 17, 1989; revised December 19, 1989)

*Cross sections / Proton-induced reactions /  
Radionuclide production / Spallation / Fragmentation /  
Accelerator mass spectrometry*

### Abstract

A large number of target elements was irradiated at accelerators in France and USA with protons of 800, 1200 and 2600 MeV. The measurements of cross sections for the production of  ${}^7\text{Be}$ ,  ${}^{10}\text{Be}$  and  ${}^{22}\text{Na}$  are described here.  ${}^7\text{Be}$  and  ${}^{22}\text{Na}$  were measured  $\gamma$ -spectrometrically,  ${}^{10}\text{Be}$  by accelerator mass spectrometry (AMS). For the preparation of the AMS-samples chemical separation methods were developed in order to allow separation of all possible reaction products of interest from only one target-foil. The new cross sections are compared with literature data and discussed with respect to the underlying production mechanisms.

### Introduction

The knowledge of cross sections of nuclear reactions is important for many fields of science. Particularly, they are needed in astrophysics and meteoritics to describe the interactions of cosmic rays with matter. Galactic and solar cosmic rays consist of about 90% protons and 10% alpha-particles [1]. Stable and radioactive nuclides produced by nuclear interactions of cosmic rays with terrestrial and extraterrestrial matter give information about various processes in the solar system. For the interpretation of production in extraterrestrial matter an exact model is necessary which can be only developed on the basis of accurate cross sections of the entire energy-region of the cosmic rays. For the galactic protons energies between 500 MeV and 10 GeV are of interest.

All nuclides produced and measured in this work are of interest as cosmogenic nuclides.  ${}^{22}\text{Na}$  is observed in lunar samples and meteorites and, moreover contributes as precursor with nearly 50% to  ${}^{22}\text{Ne}$ ,

which is an indicator for the depth of a sample inside a meteorite. It gives some information about the real volume of the meteorite before ablation in the earth's atmosphere.  ${}^{10}\text{Be}$  is a cosmogenic nuclide, which is needed for the investigation of the irradiation ages of extraterrestrial bodies and  ${}^7\text{Be}$  contributes significantly to the radioactive inventory of the earth's atmosphere [2].

In nuclear physics cross sections are necessary to understand nuclear reaction mechanisms. For low-energy reactions via a compound-nucleus reliable models were developed, e.g. by Weisskopf [3]. For preequilibrium-reactions successful models exist, e.g. Blann's hybrid-model [4]. But for high-energy reactions such as spallation- and fragmentation-reactions no satisfying model exists up to now. Here  ${}^7\text{Be}$  and  ${}^{10}\text{Be}$  are of particular importance, since the Be-isotopes should mainly be due to fragmentation, whilst  ${}^{22}\text{Na}$  from the target elements between Mg and Rh is supposed to be due to spallation. Partially, the deficit in models for high-energy reactions is based on the absence of accurate cross sections in this energy region.

The experiments described here continue a project which was started with 600 MeV proton irradiation at CERN [5] in order to improve the experimental data base for high-energy reactions. The new experiment's aim is the determination of a large number of product nuclides from target elements with masses between 16 and 196. The study comprises the measurement of radionuclides by  $\gamma$ -spectrometry and accelerator mass spectrometry as well as of stable rare gas isotopes by conventional mass spectrometry. In this article we deal with the cross sections measured for the production of  ${}^7\text{Be}$ ,  ${}^{10}\text{Be}$  and  ${}^{22}\text{Na}$  in order to elucidate two major aims of our investigations. One is to provide quantitative data for the production cross section of cosmogenic nuclides in extraterrestrial matter, the other is to discuss the differences in production mechanisms, here those between spallation and fragmentation.

## Experimental

### Irradiations

The irradiations were performed with 800 MeV protons at Los Alamos National Laboratory (LANL, USA) and with 1200 and 2600 MeV protons at Laboratoire Nationale Saturne (LNS, F). The target elements were chosen to be of interest for both, for meteoritics and for nuclear physics. For the irradiations, stacks of high purity metal foils (Mg, Al, Si, Ti, V, Fe, Co, Ni, Cu, Nb, Rh, Zr, Au) or disks of suitable chemical compositions (O as SiO<sub>2</sub>, Ca as CaF<sub>2</sub>, Mn as Mn/Ni alloy and Ba in form of a Ba-containing glass) were used. The foils had a diameter of 15.7 mm and were between 38 µm and 3.5 mm thick. For each element three foils were packed and only the one in the middle was used for the measurements, because it was not affected by recoil contamination or loss. Between the different elements there were high purity Al-foils in order to avoid cross contamination and at the same time to serve as monitor foils. The complete stacks were enclosed in containers consisting of pure aluminum. These containers allowed transport of the stacks to Germany without unpacking. The irradiation with 800 MeV protons was done for 20400 s with a proton flux of  $(8.7 \pm 0.1) \cdot 10^{10} \text{ cm}^{-2} \text{ s}^{-1}$ . The bombardments at 1200 and 2600 MeV energy were done for 39600 s and 43100 s with proton fluxes of  $(6.1 \pm 0.1) \cdot 10^{10} \text{ cm}^{-2} \text{ s}^{-1}$  and  $(2.2 \pm 0.1) \cdot 10^{10} \text{ cm}^{-2} \text{ s}^{-1}$ , respectively. These values for the fluxes are those for the first foils of each stack, and therefore do not apply to all elements, but rather are typical values. For each element-foil an individual flux was determined from the nearest Al-monitor. The fluxes were determined on the basis of the cross sections for the reaction  $^{27}\text{Al}(p,3p3n)^{22}\text{Na}$  as recommended in the evaluation of Tobailem and de Lassus St. Genies [6]. The actual cross sections adopted for 800 MeV, 1200 MeV and 2600 MeV were 15.5 mb, 14.4 mb and 11.6 mb, respectively. Since Tobailem and de Lassus St. Genies [6] did not give errors for their evaluated cross sections the errors of the flux determination were based on the experimental uncertainties of this work only (see below).

### γ-Spectrometry

The measurements of short-lived radionuclides such as  $^{24}\text{Na}$  and  $^{28}\text{Mg}$  were started at Cologne and Hannover with Ge(Li)-detectors about 40 hours after the end of irradiations in Saclay. In case of the irradiation in Los Alamos the measurements could not be started earlier than 160 hours after the end of the irradiation so short-lived radionuclides, such as  $^{24}\text{Na}$ , could be detected with low-level spectrometers for a small number of target elements only.

The measurements were supported by automatic sample changers controlled by a personal computer which accumulated the data, too. The detector ef-

iciencies were calibrated with radionuclide standards of  $^{22}\text{Na}$ ,  $^{54}\text{Mn}$ ,  $^{57}\text{Co}$ ,  $^{60}\text{Co}$ ,  $^{133}\text{Ba}$ ,  $^{137}\text{Cs}$ ,  $^{152}\text{Eu}$ ,  $^{226}\text{Ra}$  and  $^{241}\text{Am}$ . The accuracies of the standards were between 2 and 4.5%. The collected data were evaluated by special computer programs, which were developed for the problem of handling a large volume of data. The energies, branching ratios and the half-lives of the radionuclides, which were used for the evaluation of cross sections, were taken from [7, 8].

### Chemistry

After cooling of the irradiated foils the chemical separations and preparations of samples for the accelerator mass spectrometry [AMS] were done. It was necessary to separate several long-lived radionuclides from one foil. Besides the  $^{10}\text{Be}$  determined here, samples for the determination of  $^{26}\text{Al}$ ,  $^{41}\text{Ca}$  and  $^{53}\text{Mn}$  were prepared, which still wait for AMS-measurement. The carriers for all the interesting radionuclides were added before dissolving the target material. The element symbols in the brackets give the elements which were added as carrier to the target foils: SiO<sub>2</sub>(Be), Mg(Al, Be), Al(Be), Si(Al, Be), Fe(Al, Be, Ca, Mn). The separation schemes for the different target materials are as follows:

**Oxygen** [9]: The quartz disks were dissolved and evaporated with hydrofluoric acid in order to remove the Si so that finally only the beryllium fraction was left. The residue was evaporated with hydrofluoric acid and perchloric acid to remove the boron in form of BF<sub>3</sub>. The solid was dissolved in diluted hydrochloric acid and the hydroxides were precipitated with ammonia solution. The precipitate was washed with bidistilled water, centrifuged, dried and glowd to BeO.

**Magnesium** [9]: The magnesium foils were dissolved in diluted hydrochloric acid. The separation of beryllium and aluminum from the target material was carried out by precipitating the hydroxides repeatedly. The hydroxides were dissolved in hydrochloric acid, reduced to dryness and evaporated with aqua regia to remove ammonium chloride. The residue was taken up with a small amount of 1 n HCl and transferred completely to a cation-exchange column. The beryllium fraction was eluted with 1 n HCl and the aluminum fraction with 4.5 n HCl. The Be-solution was reduced and treated as described above. The aluminum fraction was reduced, evaporated with aqua regia, the hydroxides were precipitated with ammonia, washed with diluted ammonia water, dried and glowd to Al<sub>2</sub>O<sub>3</sub>.

**Aluminum**: The aluminum foils were dissolved in hydrochloric acid. The separation of aluminum and beryllium was done as described for the chemistry of magnesium, but the volume of the exchange column was larger. The fractions of the elements were treated afterwards as described above.

**Silicon** [9]: The silicon foils were dissolved in and evaporated with a mixture of nitric acid and hydrofluoric acid, so that the silicon was removed as SiF<sub>4</sub>.

The remaining aluminum and beryllium fractions were separated in the usual way.

**Iron:** The iron foils were dissolved in strong hydrochloric acid and the main part of the target material was separated by extraction with di-iso-propyl ether. The remaining ether was removed by heating and the residual iron was oxidized with hydrogen peroxide to Fe(III). This step is necessary, because otherwise Fe(II) would be treated in the following anion-exchange like Mn(II). The first 15 ml of the exchange solution consisted of aluminum, beryllium and calcium. The following fractions consisted of manganese and iron. The calcium was isolated from the two other elements by precipitating the hydroxides of beryllium and aluminum. The calcium fraction was reduced and evaporated with aqua regia. The residue was dissolved with dilute hydrochloric acid and the calcium was precipitated by adding some drops of a solution of ammonia oxalate followed by some ammonia. This precipitate was washed, dried and glowed at above  $900^\circ\text{C}$  to CaO. The separation of beryllium and aluminum was done as described above.

## AMS

The BeO powder was mixed with high purity copper powder and pressed in sample holders for the AMS measurement. The technique of AMS is described elsewhere [10]. The measurements of  $^{26}\text{Al}$  are not yet finished and the measurements of  $^{41}\text{Ca}$  are in the state of technical development.

## Results

The results of the  $^7\text{Be}$ ,  $^{10}\text{Be}$  and  $^{22}\text{Na}$  determinations are given in Tables 1 – 3.

Since it is not possible to distinguish the contributing production modes such as nuclear and complex particle emission, spallation and fragmentation reactions by integral cross section measurements the reactions are just given in the form (p, xpyn).

In Table 3 also cross sections for the reaction  $^{27}\text{Al}(p, 3p3n)^{22}\text{Na}$  are given. These cross sections were determined from aluminum target-foils using the proton fluxes derived from the next-lying aluminum catcher-foil. Thus these cross sections prove the excellent internal consistency of our cross section determination.

The errors given for the cross sections in Tables 1 – 3 consider the uncertainties in the determination of target atoms (2%), the error of the flux determination (< 3%), the uncertainties of the absolute calibration of Ge(Li)-spectrometers (< 5%) or, in case of the  $^{10}\text{Be}$ -determination, the error of the chemistry (error of the mass of the carrier material and of the graduated pipette) (3%) and the error of the AMS measurement (< 3%). Impurities of the target material were negligible. In case of  $\text{SiO}_2$  and Mn/Ni targets the contri-

**Table 1.** Cross sections for the production of  $^7\text{Be}$

Reaction	Cross section [mb] at		
	800 MeV	1200 MeV	2600 MeV
$\text{O}_{\text{nat}}(p, 5p\text{xn})^7\text{Be}$	11.0 $\pm 0.9$	11.7 $\pm 0.9$	9.41 $\pm 0.75$
$\text{Mg}_{\text{nat}}(p, 9p\text{xn})^7\text{Be}$	7.88 $\pm 0.64$	9.92 $\pm 0.74$	9.82 $\pm 0.71$
$^{27}\text{Al}(p, 10p11n)^7\text{Be}$	5.98 $\pm 0.43$	8.36 $\pm 0.61$	8.65 $\pm 0.62$
$\text{Si}_{\text{nat}}(p, 11p\text{xn})^7\text{Be}$	7.57 $\pm 0.62$	10.1 $\pm 0.7$	10.8 $\pm 0.8$
$\text{Ti}_{\text{nat}}(p, 19p\text{xn})^7\text{Be}$	3.19 $\pm 0.24$	4.80 $\pm 0.37$	6.94 $\pm 0.54$
$\text{V}_{\text{nat}}(p, 20p\text{xn})^7\text{Be}$	4.14 $\pm 0.32$	5.98 $\pm 0.44$	6.58 $\pm 0.59$
$^{55}\text{Mn}(p, 22p27n)^7\text{Be}$	2.84 $\pm 0.25$	5.03 $\pm 0.41$	7.41 $\pm 0.63$
$\text{Fe}_{\text{nat}}(p, 23p\text{xn})^7\text{Be}$	3.12 $\pm 0.23$	5.26 $\pm 0.40$	8.33 $\pm 0.61$
$^{59}\text{Co}(p, 24p29n)^7\text{Be}$	2.58 $\pm 0.21$	4.49 $\pm 0.33$	7.32 $\pm 0.57$
$\text{Ni}_{\text{nat}}(p, 25p\text{xn})^7\text{Be}$	3.77 $\pm 0.30$	5.82 $\pm 0.44$	9.84 $\pm 0.72$
$\text{Cu}_{\text{nat}}(p, 26p\text{xn})^7\text{Be}$	2.62 $\pm 0.21$	4.17 $\pm 0.30$	6.93 $\pm 0.50$
$^{93}\text{Nb}(p, 38p49n)^7\text{Be}$	2.30 $\pm 0.24$	3.88 $\pm 0.30$	7.28 $\pm 0.56$
$\text{Zr}_{\text{nat}}(p, 37p\text{xn})^7\text{Be}$	2.32 $\pm 0.31$	3.70 $\pm 0.32$	6.41 $\pm 0.52$

**Table 2.** Cross sections for the production of  $^{10}\text{Be}$

Reaction	Cross section [mb] at		
	800 MeV	1200 MeV	2600 MeV
$\text{O}_{\text{nat}}(p, 5p\text{xn})^{10}\text{Be}$	2.77 $\pm 0.17$	3.44 $\pm 0.21$	2.55 $\pm 0.15$
$\text{Mg}_{\text{nat}}(p, 9p\text{xn})^{10}\text{Be}$	1.96 $\pm 0.12$	2.45 $\pm 0.15$	2.89 $\pm 0.17$
$^{27}\text{Al}(p, 10p8n)^{10}\text{Be}$	2.10 $\pm 0.13$	3.01 $\pm 0.18$	3.02 $\pm 0.18$
$\text{Si}_{\text{nat}}(p, 11p\text{xn})^{10}\text{Be}$	1.39 $\pm 0.08$	2.02 $\pm 0.13$	2.38 $\pm 0.14$
$\text{Fe}_{\text{nat}}(p, 23p\text{xn})^{10}\text{Be}$	1.03 $\pm 0.06$	1.86 $\pm 0.11$	3.45 $\pm 0.21$

butions of Si and Ni were corrected by using the respective cross sections measured in this work. Recoil-loss or -contamination were negligible, because always the foils in the middle of each element-stack were taken for the analysis. A more detailed discussion of the

**Table 3.** Cross sections for the production for  $^{22}\text{Na}$ 

Reaction	Cross section [mb] at		
	800 MeV	1200 MeV	2600 MeV
$\text{Mg}_{\text{nat}}(\text{p},2\text{p}\text{xn})^{22}\text{Na}$	29.7 $\pm 2.1$	28.9 $\pm 2.1$	23.7 $\pm 1.7$
$^{27}\text{Al}(\text{p},3\text{p}3\text{n})^{22}\text{Na}$	15.6 $\pm 1.1$	14.6 $\pm 1.0$	11.4 $\pm 0.8$
$\text{Si}_{\text{nat}}(\text{p},4\text{p}\text{xn})^{22}\text{Na}$	19.6 $\pm 1.4$	18.9 $\pm 1.3$	14.5 $\pm 1.0$
$\text{Ca}_{\text{nat}}(\text{p},10\text{p}\text{xn})^{22}\text{Na}$	5.87 $\pm 0.44$	7.14 $\pm 0.53$	5.92 $\pm 0.45$
$\text{Ti}_{\text{nat}}(\text{p},12\text{p}\text{xn})^{22}\text{Na}$	1.60 $\pm 0.12$	2.64 $\pm 0.19$	3.04 $\pm 0.25$
$\text{V}_{\text{nat}}(\text{p},13\text{p}\text{xn})^{22}\text{Na}$	1.67 $\pm 0.12$	2.42 $\pm 0.17$	2.62 $\pm 0.26$
$^{55}\text{Mn}(\text{p},15\text{p}19\text{n})^{22}\text{Na}$	0.742 $\pm 0.072$	1.54 $\pm 0.12$	2.35 $\pm 0.22$
$\text{Fe}_{\text{nat}}(\text{p},16\text{p}\text{xn})^{22}\text{Na}$	0.780 $\pm 0.061$	1.62 $\pm 0.12$	2.52 $\pm 0.20$
$^{59}\text{Co}(\text{p},17\text{p}21\text{n})^{22}\text{Na}$	0.475 $\pm 0.062$	1.18 $\pm 0.08$	2.15 $\pm 0.17$
$\text{Ni}_{\text{nat}}(\text{p},18\text{p}\text{xn})^{22}\text{Na}$	0.676 $\pm 0.097$	1.52 $\pm 0.11$	2.74 $\pm 0.23$
$\text{Cu}_{\text{nat}}(\text{p},19\text{p}\text{xn})^{22}\text{Na}$	0.335 $\pm 0.051$	0.808 $\pm 0.058$	1.75 $\pm 0.13$
$\text{Zr}_{\text{nat}}(\text{p},30\text{p}\text{xn})^{22}\text{Na}$		0.191 $\pm 0.032$	
$^{93}\text{Nb}(\text{p},31\text{p}41\text{n})^{22}\text{Na}$			0.82 $\pm 0.14$
$^{103}\text{Rh}(\text{p},35\text{p}47\text{n})^{22}\text{Na}$			0.82 $\pm 0.12$

various sources of errors affecting the experimental determination of cross sections, which also is valid for this work, was given earlier [5].

In Figures 1–7 the new data are compared with some literature data. In these figures no errors are given for better legibility. A comparison of our new data now shall be done, considering the entire excitation functions up to 10 GeV. We will, however, totally neglect in this discussion the data of Rayudu [11, 12] which from our experience mostly are insufficient and are in contradiction to all newer cross section measurements.

For the reaction  $\text{O}(\text{p},5\text{p}\text{xn})^7\text{Be}$ , there is a relatively good agreement (Figure 1) between our new data and the earlier determinations [5, 13, 14, 15, 16] between 600 MeV and 6000 MeV. It should be mentioned, however, that the cross section given by Raisbeck and Yiou [14] at 1000 MeV is lower than our data at 800 and 1200 MeV by 15–20%. In spite of this discrepancy, above 600 MeV the excitation function now is well established. At lower energies, however, first there are only some contradictory data by Heydegger *et al.*

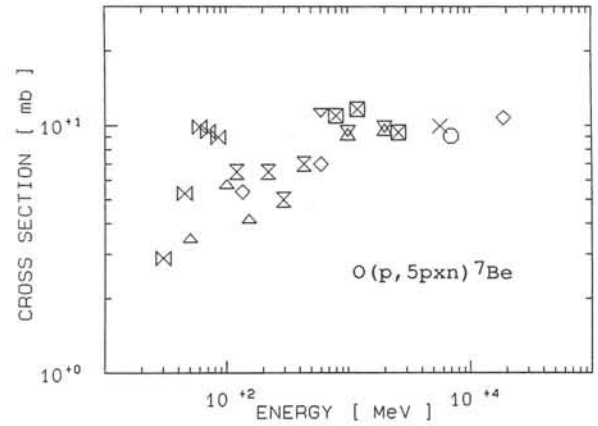


**Fig. 1.** Excitation function for the reaction  $\text{O}(\text{p},5\text{p}\text{xn})^7\text{Be}$  as revealed by the cross sections from this work ( $\blacksquare$ ) and by earlier data ( $\nabla$ =[5],  $\times$ =[13],  $\boxtimes$ =[14],  $\diamond$ =[15],  $\circ$ =[16],  $\boxtimes$ =[17],  $\triangle$ =[18],  $\boxtimes$ =[19]).

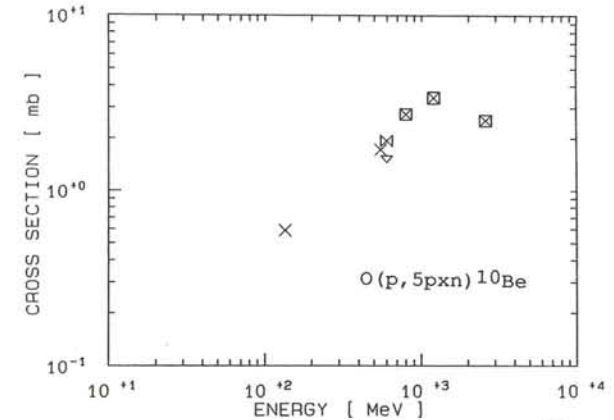


**Fig. 2.** Excitation function for the reaction  $\text{O}(\text{p},5\text{p}\text{xn})^{10}\text{Be}$  as revealed by the cross sections from this work ( $\blacksquare$ ) and by earlier data ( $\nabla$ =[5],  $\times$ =[20],  $\boxtimes$ =[21]).

[17] between 160 and 600 MeV. Secondly, the data below 150 MeV [15, 17, 18, 19] show some ambiguity. In particular, the data of Lafleur *et al.* [19] and Bimbot [18] do not fit together. Here some more additional measurements are required.

For the reaction  $\text{O}(\text{p},5\text{p}\text{xn})^{10}\text{Be}$  data exist by some authors [5, 20, 21] between 100 and 2600 MeV (Figure 2). But below 600 MeV there is only one determination at 135 MeV [20]. The data allow to estimate the general shape of the excitation function. But more data in the low-energy region are necessary. Around 600 MeV the data by Michel *et al.* [5] ( $1.52 \pm 0.15$ ) mb, Raisbeck and Yiou [21] with ( $1.94 \pm 0.36$ ) mb and Amin *et al.* [20] at 550 MeV with ( $1.72 \pm 0.1$ ) mb are in reasonable agreement.

There is a very good agreement between the results of various authors [5, 14, 17, 18, 22, 23] who investigated the reaction  $\text{Mg}(\text{p},9\text{p}\text{xn})^7\text{Be}$ . An unambiguous excitation function can be plotted (Figure 3) between 50 and 30000 MeV.

A similar quality would be desirable also for the reaction  $\text{Mg}(\text{p},9\text{p}\text{xn})^{10}\text{Be}$ , which is of particular im-

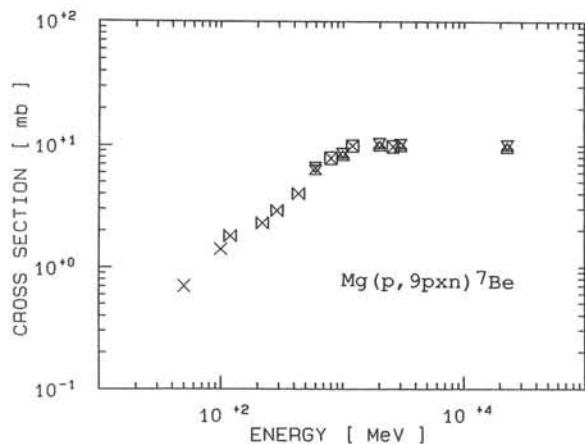


**Fig. 3.** Excitation function for the reaction  $\text{Mg}(p,9\text{pxn}){}^7\text{Be}$  as revealed by the cross sections from this work ( $\blacksquare$ ) and by earlier data ( $\nabla$ =[5],  $\Delta$ =[14],  $\triangleright$ =[17],  $\times$ =[18],  $\boxtimes$ =[22],  $\boxplus$ =[23]).

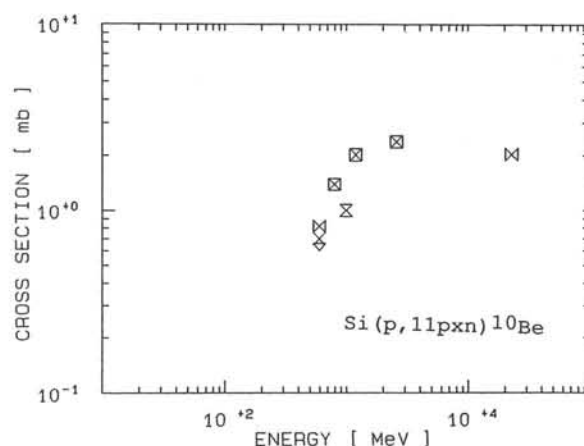


**Fig. 5.** Excitation function for the reaction  $\text{Si}(p,11\text{pxn}){}^{10}\text{Be}$  as revealed by the cross sections from this work ( $\blacksquare$ ) and by earlier data ( $\nabla$ =[5],  $\triangleright$ =[21],  $\times$ =[33],  $\boxplus$ =[34]).

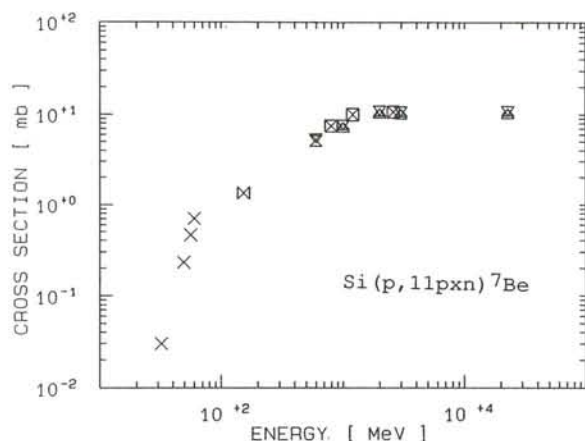


**Fig. 4.** Excitation function for the reaction  $\text{Si}(p,11\text{pxn}){}^7\text{Be}$  as revealed by the cross sections from this work ( $\blacksquare$ ) and by earlier data ( $\nabla$ =[5],  $\Delta$ =[14],  $\triangleright$ =[18],  $\boxtimes$ =[22],  $\boxplus$ =[23],  $\times$ =[32]).

portance for meteoritics. But for this reaction only the measurements at 600 MeV by Michel *et al.* [5] with  $(1.03 \pm 0.09)$  mb and by Raisbeck and Yiou [21] with  $(1.27 \pm 0.33)$  mb exist beside our new data. Here again measurements at lower energies are needed.

A large number of data exists below 500 MeV for the reaction  $\text{Mg}(p,2\text{pxn}){}^{22}\text{Na}$  [24, 25]. However, they still show strong discrepancies for energies below 100 MeV, which should be further investigated. Above 500 MeV the data from this work, together with the data of Michel *et al.* [5], Raisbeck and Yiou [14, 22] and Baros and Regnier [26] give a consistent excitation function.

For the reactions  $\text{Al}(p,10\text{p}11\text{n}){}^7\text{Be}$  and  $\text{Al}(p,3\text{p}3\text{n}){}^{22}\text{Na}$  a large number of data exists in literature, see for references [6, 27, 28, 29, 30, 31]. These cross sections cannot be displayed in a figure because too many data exist. Our data fit the excitation functions very well.

For  $\text{Al}(p,10\text{p}8\text{n}){}^{10}\text{Be}$  exclusively our group's measurements for production cross sections (this work and

[5]) exist. Here more data are needed, also by other authors, in particular because the ratios  ${}^{10}\text{Be}/{}^7\text{Be}$  and  ${}^{10}\text{Be}/{}^{22}\text{Na}$  from Al would allow to better investigate the accuracy of  ${}^{10}\text{Be}$  determinations, since evaluated excitation functions for  $\text{Al}(p,10\text{p}11\text{n}){}^7\text{Be}$  and  $\text{Al}(p,3\text{p}3\text{n}){}^{22}\text{Na}$  minimize the flux monitoring problems.

There is a relatively large number of data available for the reaction  $\text{Si}(p,11\text{pxn}){}^7\text{Be}$  [5, 14, 18, 22, 23, 32], which describe the excitation function of the reaction fairly well (Figure 4). There are only some further data necessary between 200 and 600 MeV and between 60 and 130 MeV.

Besides the new data of  $\text{Si}(p,11\text{pxn}){}^{10}\text{Be}$  other cross sections were reported by [5, 21, 33, 34] (Figure 5). There are no data available below 600 MeV, which are highly desirable, considering the importance of Si as cosmic target element. At 600 MeV there is still some scatter of the data, the actual cross sections agreeing, however,  $(0.630 \pm 0.204)$  mb [5],  $(0.760 \pm 0.3)$  mb [33] and  $(0.82 \pm 0.20)$  mb [21] within the limits of error. The measurement by Dedieu [34] at 1 GeV with  $(1.0 \pm 0.2)$  mb is considerably lower than the indicated trend of our new data.

For the excitation function for the reaction  $\text{Si}(p,4\text{pxn}){}^{22}\text{Na}$  there is a lot of data (see for references [6]). But most of the data between 130 and 600 MeV are from the work by Rayudu [11, 12], so that there are some more data needed in this energy region.

For the reaction  $\text{Fe}(p,23\text{pxn}){}^7\text{Be}$  again a consistent excitation function exists (Figure 6), containing data from this work as well as from [5, 14, 22, 35, 36, 37, 38]. For a better description of the threshold of this reaction some more measurements below 600 MeV are desirable.

For the production of  ${}^{10}\text{Be}$  from iron (Figure 7) the earlier data by Michel *et al.* [5] at 600 MeV with  $(0.58 \pm 0.04)$  mb and by Honda and Lal [40] at 720 MeV with 1.2 mb fit well to the shape of the excitation function indicated by our new data. Low energy

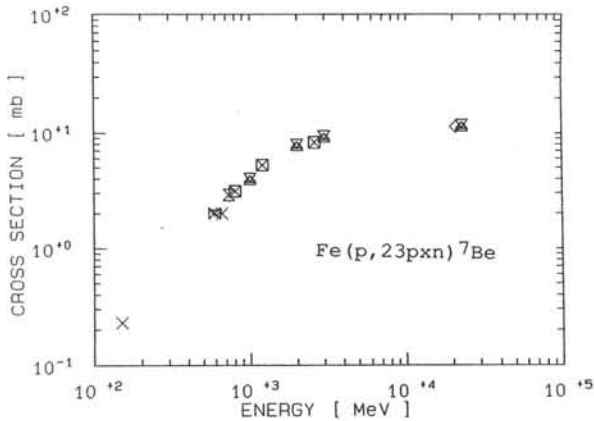


Fig. 6. Excitation function for the reaction  $\text{Fe}(p,23pxn)^7\text{Be}$  as revealed by the cross sections from this work ( $\blacksquare$ ) and by earlier data ( $\nabla$ =[5],  $\triangle$ =[14],  $\boxtimes$ =[22],  $\times$ =[35],  $\blacktriangleleft$ =[36],  $\boxtimes$ =[37],  $\diamond$ =[38]).

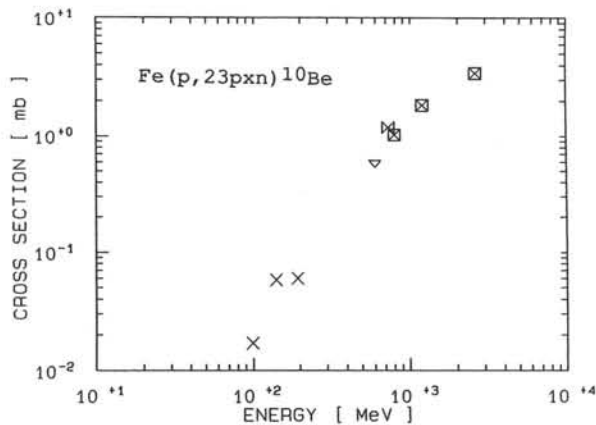


Fig. 7. Excitation function for the reaction  $\text{Fe}(p,23pxn)^{10}\text{Be}$  as revealed by the cross sections from this work ( $\blacksquare$ ) and by earlier data ( $\nabla$ =[5],  $\times$ =[39],  $\blacktriangleleft$ =[40]).

data were only measured by Theis [39] between 99 and 194 MeV, so that more measurements are necessary, in particular for the modelling of  $^{10}\text{Be}$  in iron meteorites.

Finally, the reaction  $\text{Fe}(p,16pxn)^{22}\text{Na}$  can be considered well known now. The new data close the gaps and agree well with the earlier data (see [5] for a detailed discussion).

## Discussion

Here we will not go into details of model calculations for cosmogenic nuclides, but rather will discuss some aspects of the reaction mechanisms being of importance for the production of the three product nuclides. As pointed out above there is no adequate model describing proton-induced high-energy reactions. Several attempts have been made to describe the cross sections of high-energy reactions by semiempirical formulae [41, 42, 43, 44]. The formulae by Rudstam [41] and Silberberg and Tsao [42] turned out to be widely unreliable and only to represent the general trends of high-energy cross sections. It is not clear up

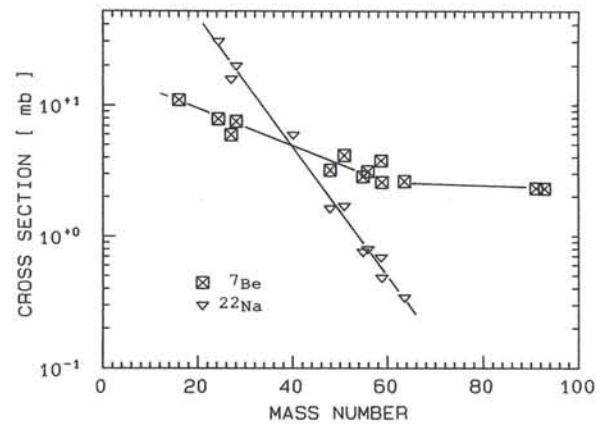


Fig. 8. Dependence on target mass number of cross sections for the production of  $^7\text{Be}$  and  $^{22}\text{Na}$  at 800 MeV protons ( $\blacksquare$  =  $^7\text{Be}$ ,  $\nabla$  =  $^{22}\text{Na}$ ).

to now, whether the deficits of these approaches are due to these authors using an at that time insufficient data base. A detailed analysis of their formulae on the basis of our work [5, 45] showed that one has to account for discrepancies between calculated and experimental data of one order of magnitude. It will be highly desirable to evaluate the capabilities of semiempirical formulae using the new data for the determination of the parameter of these formulae, in order to get rid of the bias of unreliable data in such an approach. This will be soon done for the newer formulae [43, 44].

Another more physical approach is based on the two-step-model of Serber [46], describing high-energy reactions by a quick initial knock-on phase dominated by nucleon-nucleon interactions followed by a slow deexcitation, which is described by the decay of a residual compound nucleus according to the statistical model of nuclear reactions. Such model calculations can be done by the Monte Carlo codes, as e.g. HETC [47]. First, calculations for the target element iron [5] were promising. A systematic study is presently performed. However, these calculations up to now do neither describe fragmentation nor do they include moderate excitation energies between the high-energy knock-on phase and the low-energy evaporation.

The nuclides dealt with within this study are of particular interest, since they allow to describe the transition from spallation to fragmentation. The dependence on target mass numbers of the production cross sections of  $^7\text{Be}$  and  $^{22}\text{Na}$  is given in the Figures 8–10.

As far as data are available,  $^{10}\text{Be}$  turns out to behave exactly like  $^7\text{Be}$ . Thus all conclusions about the differences in the production modes of  $^7\text{Be}$  and  $^{22}\text{Na}$  also apply to the nuclide pairs  $^{10}\text{Be}$  and  $^{22}\text{Ne}$ . According to the systematics of spallation reactions as described by Serber's two-step-model, the isobaric yields should decrease exponentially with the mass difference between the target and the product. Here the production cross sections of  $^{22}\text{Na}$  and  $^7\text{Be}$  do

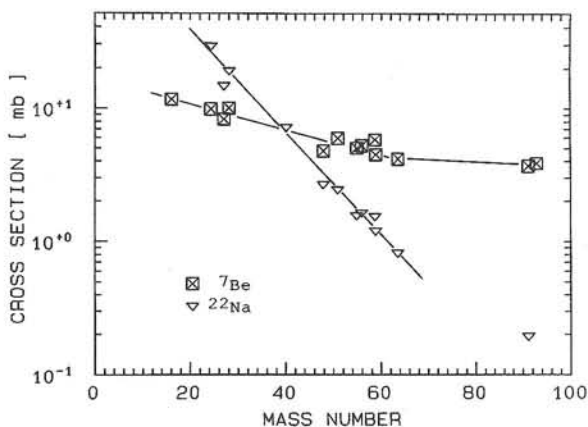


Fig. 9. Dependence on target mass number of cross sections for the production of  ${}^7\text{Be}$  and  ${}^{22}\text{Na}$  at 1200 MeV protons ( $\square = {}^7\text{Be}$ ,  $\nabla = {}^{22}\text{Na}$ ).

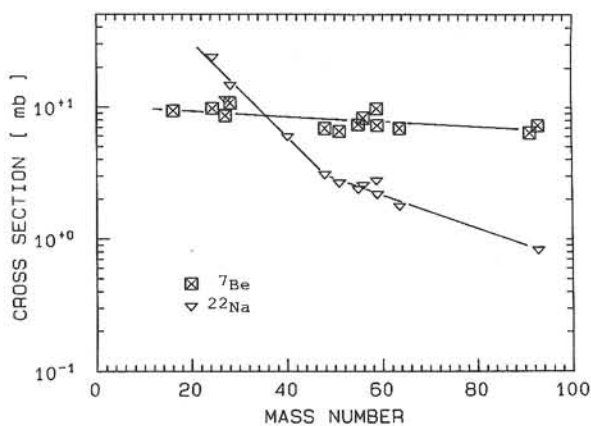


Fig. 10. Dependence on target mass number of cross sections for the production of  ${}^7\text{Be}$  and  ${}^{22}\text{Na}$  at 2600 MeV protons ( $\square = {}^7\text{Be}$ ,  $\nabla = {}^{22}\text{Na}$ ).

account for nearly half of the isobaric yields for the masses 22 and 7, respectively. In contrast to fragmentation, when the product is emitted as a large complex entity from the target nucleus, a pure spallation product is believed to be the residual of a sequence of quickly emitted knock-on particles and of an evaporation period. As Figures 8 and 9 display for  ${}^{22}\text{Na}$  for 800 and 1200 MeV the cross sections decrease by more than two orders of magnitude exponentially with increasing mass numbers of the targets and thereby with increasing mass differences between target and product.

The data for  ${}^7\text{Be}$ , on the other hand, vary by less than a factor of 10 at 800 and 1200 MeV. At 2600 MeV they differ even by less than 30%. Though for  ${}^7\text{Be}$  the differences between target and product masses are much larger than for  ${}^{22}\text{Na}$ , the slopes for the eyeguiding lines in Figure 8–10 are much smaller than for  ${}^{22}\text{Na}$ . This shows that both nuclides are produced by strongly different reaction mechanisms.

There is, however, an indication that the production of  ${}^{22}\text{Na}$  is changing the mechanism when go-

ing to higher energies (Figure 10). The change in slopes at 2600 MeV and at mass numbers  $\approx 55$  indicates a possible production of  ${}^{22}\text{Na}$  even as fragmentation product for heavier targets.

A detailed HETC analysis will be performed in the future to elucidate these questions. The trend to smaller variations of  ${}^7\text{Be}$  production rates with target mass and with increasing energies points to a saturation effect in fragmentation and an equilibration of product yields.

#### Acknowledgement

This work was supported by the Deutsche Forschungsgemeinschaft. The authors wish to thank the collaborators at LNS and LANL for the assistance of the irradiations and the Wacker Chemietronic, Burghausen, for placing the silicon-wafers at our disposal.

#### References

1. Alsmiller Jr., R. G., *et al.*: ORNL-RSIC-35 (1972).
2. Ionising Radiation: Sources and Effects; Edt.: United Nations Scientific Committee on the effects of atomic radiation, United Nations, New York 1982.
3. Weisskopf, V.: Phys. Rev. **52**, 295 (1937).
4. Blann, M.: Phys. Rev. Lett. **27**, 337 (1971).
5. Michel, R., *et al.*: Analyst **114**, 287–293 (1989).
6. Tobaillem, J., de Lassus St. Genies, C. H.: Additif No. 2 a la CEA-N-1466(1) (1975), CEA-N-1466(4) (1977), CEA-N-1466(5) (1981).
7. Seelmann-Eggebert, W., *et al.*: *Karlsruher Nuklidkarte*, 5th Edt. 1981, Gersbach und Sohn, München.
8. Reus, U., Westmeier, W.: At. Data Nucl. Data Tables **29**, 1–192 and 193–406 (1983).
9. Theis, St., Englert, P.: J. Radioanal. Nucl. Chem. **110**, 1, 203–214 (1986).
10. Suter, M., *et al.*: Nucl. Instr. Meth. in Phys. Res. **B5**, 117–122 (1984).
11. Rayudu, G. V. S.: Can. J. Chem. **42**, 1149–1154 (1964).
12. Rayudu, G. V. S.: J. Inorg. Chem. **30**, 3211–3219 (1968).
13. Benioff, P. A.: Phys. Rev. **119**, 316–324 (1960).
14. Raisbeck, G. M., Yiou, F.: Proc. 14th Int. Cosmic Ray Conf., Munich, Vol. 2, 495 (1975).
15. Yiou, F., *et al.*: J. Geophys. Res., Space Research **74**, 2447–2448 (1969).
16. Stapleton, G. B., Thomas, R. H.: Nucl. Phys. **A175**, 124–128 (1971).
17. Heydegger, H. R., *et al.*: Phys. Rev. **C14**, 1506–1514 (1976).
18. Bimbot, G.: Compt. Rend. Ser. **B272**, 1054–1057 (1971).
19. Lafleur, M. S., *et al.*: Can. J. Chem. **44**, 2749–2767 (1966).
20. Amin, B. S., *et al.*: Nucl. Phys. **A195**, 311–320 (1972).
21. Raisbeck, G. M., *et al.*: 15th Int. Cosmic Ray Conf., Plovdiv, Vol. 2, 203–207 (1977).
22. Raisbeck, G. M., Yiou, F.: Phys. Rev. **C12**, 915–920 (1975).
23. Raisbeck, G. M., Yiou, F.: Phys. Rev. **C9**, 1385–1395 (1974).
24. Bartell, F. O., Softky, S.: Phys. Rev. **84**, 463–465 (1951).
25. Batzel, R. E., Coleman, G. H.: Phys. Rev. **91**, 280–282 (1954).
26. Baros, F., Regnier, S.: J. Phys. (Paris) **45**, 855–861 (1984).
27. McGowan, F. K., Milner, W. T.: At. Data Nucl. Data Tables **18**, 1 (1976).
28. Burrows, T. W., Demsey, P.: *The Bibliography of Integral Charged Particles Nuclear Data*, Archival Edition, Parts 1 and 2, BNL-NCS-50640, Fourth Edition, National Techni-

- cal Information Service, US Department of Commerce, Springfield, VA, 1980.
29. Burrows, T. W., Wyant, G.: Suppl. 1 to [28], 1981.
30. Holden, N. E., Burrows, T. W.: Suppl. 2 to [28], 1982.
31. Holden, N. E., *et al.*: *Integral Charged Particle Nuclear Data Bibliography*, BNL-NCS-51771, National Technical Information Service, US Department of Commerce, Springfield 1985.
32. Sheffey, D. W., *et al.*: Phys. Rev. **172**, 1094–1098 (1968).
33. Raisbeck, G. M., Yiou, F.: 13th Int. Cosmic Ray Conf., Denver, Vol. 1, 494 (1973).
34. Dedieu, J.: Thesis, Bordeaux (1979).
35. Lavrukhina, A. K., *et al.*: Soviet Phys., JETP **17**, 960–964 (1963).
36. Orth, C. J., *et al.*: J. Inorg. Nucl. Chem. **38**, 13–17 (1976).
37. Honda, M., Lal, D.: Phys. Rev. **118**, 1618–1625 (1960).
38. Perron, C.: Phys. Rev. **C14**, 1108–1120 (1976).
39. Theis, St.: Thesis, Universität zu Köln (1986).
40. Honda, M., Lal, D.: Nucl. Phys. **51**, 363–368 (1964).
41. Rudstam, G.: Z. Naturforsch. **21a**, 1027–1041 (1966).
42. Silberberg, R., Tsao, C. H.: Astrophys. J. Suppl. **25**, 315–333 (1973).
43. Sümmerer, K.: GSI-Nachrichten 07-89, 10–14 (1989).
44. Sauvanion, H.: Z. Phys. A-Atomic Nuclei **326**, 301–308 (1987).
45. Dittrich, B., *et al.*: NEANDC(E)-302 V, 31–41 (1989).
46. Serber, R.: Phys. Rev. **72**, 1114–1115 (1947).
47. Cloth, P., *et al.*: Jül. Spez. **196** (1983) ISSN 0343-7639.